A method for data processing to obtain high quality XCTD data

Hiroshi Uchida[1,*], Koji Shimada[2], and Takeshi Kawano[1]

[1]Research Institute for Global Change, Japan Agency for Marine-Earth Science and Technology, Kanagawa, Japan

[2]Department of Ocean Sciences, Faculty of Marine Science, Tokyo University of Marine Science and Technology, Tokyo, Japan

*Corresponding author: Hiroshi Uchida, Research Institute for Global Change, Japan Agency for Marine-Earth Science and Technology, 2-15 Natsushima, Yokosuka, Kanagawa 237-0061, Japan. email: huchida@jamstec.go.jp

Abstract

A data processing method for an expendable conductivity-temperature-depth profiler (XCTD) to obtain high quality XCTD data is proposed. By adjusting the mismatch of the response time of the temperature and conductivity sensors, systematic error (on the order of –0.05) in XCTD salinity data can be eliminated in a region having a strong vertical temperature gradient (>0.2 °C m^{-1}), such as in the main thermocline of the nearshore side of the Kuroshio axis and in the seasonal thermocline in the subarctic North Pacific. The systematic errors in XCTD depth data from two cruises were evaluated by comparing CTD and XCTD data taken simultaneously during each cruise. The XCTD depths were in good agreement with the CTD depths from one cruise, but depth-dependent depth errors from the other cruise were found. The cause of the depth error is unknown but may have occurred because the terminal velocity for the XCTD probes was much less (–0.0428 m s^{-1}) than that provided by the manufacturer for the later cruise. The results suggest that XCTD and expendable bathythermograph (XBT) observations may have a similar depth error, because XBT and XCTD do not have pressure sensors and therefore depth is inferred from the fall rate of the probe. Simultaneous CTD observations are required to evaluate the XBT/XCTD depth error.

1. Introduction

Since the 1960s, the expendable bathythermograph (XBT) has been widely used globally to measure upper ocean thermal structures (e.g., Wijffels et al. 2008), and since the 1990s, upper ocean salinity structures have been measured by using an expendable conductivity–temperature–depth profiler (XCTD) (e.g., Johnson 1995; Uehara et al. 2008). Although XBT/XCTD data can be easily collected from research vessels and other ships on a voluntary basis, systematic error can be a problem because the XBT and XCTD do not have pressure sensors and therefore depth is inferred from the fall rate of the probe. In addition, post-cruise calibration of temperature and conductivity sensors is not possible for expendable instruments. For example, Gouretski and Koltermann (2007) suggested that the global XBT dataset has a time-varying warm bias, and Wijffels et al. (2008) demonstrated this to be largely due to changes in the fall rate of the XBT probes.

To use XBT/XCTD data for climate change research, we must apply data processing and quality control measures that go beyond the manufacturer's specifications. In this study, we propose a data processing method for obtaining high quality XCTD data. The method eliminates systematic error in XCTD salinity data that is due to the mismatch of the response time of the temperature and conductivity sensors. We also evaluated systematic error in XCTD depth data by comparing the data to simultaneously measured CTD data.

2. Materials

We used TSK XCTD-1 and XCTD-2 probes (Tsurumi-Seiki Co. Ltd., Kanagawa, Japan) for this study. The nominal uncertainties for the two probes, as specified by the manufacturer, are listed in Table 1. The fall-rate equation provided by the manufacturer was used to infer depth (Z in meters):

$$Z = at - bt^2, \tag{1}$$

where t is the elapsed time in seconds from probe entry into the water, and a (terminal velocity) and b (acceleration) are the empirical coefficients (Mizuno and Watanabe 1998; Koso et al. 2005) (Table 2). The data sampling interval was 0.04 s.

XCTD data were obtained during the R/V Hakuho-maru cruise KH-02-3 leg 1 (15–20 September 2002) (Uchida et al. 2008) and the R/V Mirai cruises MR07-04 (12–14 August 2007) (Kawano et al. 2009) and MR09-01 leg 1 and 2 (21 April–14 June 2009) (Murata et al. 2009). XCTD data were acquired with the MK-130 data acquisition system (Tsurumi-Seiki Co., Ltd.) for the KH-02-3 and MR09-01 cruises and with the MK-100 data acquisition system (Tsurumi-Seiki Co., Ltd.) for the MR07-0 4 cruise. The number and location of XCTD casts are shown in Fig. 1.

We used an SBE 9*plus* CTD system (Sea-Bird Electronics, Inc., Bellevue, WA) as the comparative system on these cruises. The CTD pressure sensors were calibrated before each cruise against a dead-weight piston gauge (Bundenberg Gauge Co. Ltd., Manchester, UK), and the CTD temperature sensors were calibrated in situ against a Sea-Bird Electronics (SBE 35) deep ocean reference thermometer (Uchida et al. 2007) for the R/V Mirai cruises. For the R/V Hakuho-maru cruise, the CTD pressure and temperature sensors were calibrated before the cruise by the manufacturer. The CTD salinity data were corrected using the in situ water sample data. Salinity measurements for the water samples were conducted with a Guildline Autosal model 8400B salinometer (Guildline Instruments Ltd., Ontario, Canada) for the R/V Mirai cruises and with a Guildline Portasal model 8410A salinometer for the R/V Hakuho-maru cruise. The salinometers were standardized with International Association for Physical Science of the Ocean (IAPSO) Standard Seawater. The batch-to-batch differences in recent batches from P130 to P150 of the standard seawater were less than 0.001 (Kawano et al. 2006).

Simultaneous observations using the XCTD and CTD probes were carried out during cruises KH-02-3 and MR09-01, except for the easternmost five casts of cruise MR09-01. The XCTD probes were usually launched about 10 min after the start of CTD measurements. For cruise MR07-04, XCTD observations were carried out between the CTD stations. CTD data averaged over 1-dbar intervals were used for comparing to the XCTD data.

3. Data processing

a. Data processing sequence

Processing and quality control of the XCTD data were based on a method described in Uchida and Imawaki (2008) with slight modification. The data processing sequence used in the reduction of XCTD data was as follows:

1) Raw temperature and conductivity data from the first 32 scans (about 4.3 m) of the XCTD data were deleted to remove the effect of the start-up transient change (Kizu and Hanawa 2002) of XCTD measurements. Data were also deleted after the probe made contact with the bottom. Spikes in the temperature and conductivity profiles were

manually removed. Gaps caused by the deletion of data were linearly interpolated when the data gap was within 15 scans (about 2 m).

2) Temperature and conductivity data were low-pass filtered using the running mean filter with a window of 15 scans (about 2 m).
3) Conductivity data were advanced by 1.5 scans (about 0.2 m), instead of 2 scans as described in Uchida and Imawaki (2008), relative to the temperature data to correct the mismatch in response time of the sensors.
4) Salinity was calculated from pressure, temperature, and conductivity data. The pressure data were calculated by using the relation between hydrostatic pressure and depth.
5) The data were sampled at 1-dbar or 1-m intervals.
6) Salinity biases of the XCTD data were estimated by comparing temperature and salinity relationships in the deep ocean obtained from the CTD and XCTD data and the estimated salinity biases were subtracted from the original XCTD salinity data.

The data processing procedures for steps 2)–4) and 6) above are described in detail in the following subsections.

b. Noise reduction

The manufacturer's data processing software interpolates and samples XCTD temperature and salinity data at 1-m intervals to reduce the size of the data set. Salinity data is low-pass filtered using the running mean filter with a window of 13 scans (about 1.7 m) before interpolation to reduce salinity noise. However, distinct spectral spikes present in not only conductivity profiles but also temperature profiles at frequencies of 5 and 10 Hz, corresponding to 1 and 2 cycles per five scans (Gille et al. 2009). Low-pass filtered data by using the filters of Gille et al. (2009) is biased (1 mK for temperature and 0.01 for salinity) because the sum of the coefficients does not equal one. All coefficients should be multiplied by a factor of 0.9997 (1.0003) for the 21 (11)-point filter to eliminate the biases. Although the filters of Gille et al. (2009) can remove the anomalous spikes from the XCTD temperature and conductivity data, the XCTD data is still noisy compared to the CTD data averaged over 1-dbar intervals. Using a running mean filter with a window of 15 scans (about 2 m) for both of the XCTD temperature and conductivity data can effectively remove the noise (Fig. 2). The difference between the XCTD and CTD temperature–salinity profiles was 0.0058, 0.0040, and 0.0026 for the raw data, data with the anomalous spikes removed, and data subjected to a low-pass filter by using the running mean with a window of 15 scans, respectively, for the temperature range between 4.5 and 12.0 °C.

c. Correction of mismatch in response times

Time constants of the XCTD temperature and conductivity sensors were reported to be the same (0.1 s or less) (Mizuno and Watanabe 1998). However, temperature–salinity profiles measured by the XCTD often show a loop shape in the main thermocline of the Kuroshio due to a mismatch in the response times of the sensors. This mismatch was examined by using the XCTD data obtained from the nearshore side of the Kuroshio axis during cruise KH-02-3 (Fig. 1). Since the conductivity sensor is sensitive to changes in temperature, conductivity and temperature data are related. In a region with a strong vertical temperature gradient (0.2 °C m^{-1}), however, the conductivity data changes one to two scans prior to the temperature data due to a faster response time of the conductivity sensor (Fig. 3). This slight mismatch in the response times causes a large artificial fluctuation in the calculated salinity data (about 0.05) that is not seen in the CTD salinity data (Fig. 4). The mismatch can be effectively compensated for by advancing the conductivity data in time relative to the temperature data. For this example, the correlation coefficient was higher than 0.9994 after advancing the conductivity data by from 1.25 to 1.5 scans. The advance of about 1.5 scans simply resulted in less artificial fluctuation in the calculated salinity data (Fig. 4). The corrected conductivity data (C') at a scan number i can be calculated from the following equation:

$$C'_i = 0.5\,(C_{i-1} + C_{i-2}), \quad (2)$$

where C is the original conductivity data.

Using the example of the nearshore side of the Kuroshio axis, the salinity error caused by the mismatch in response times is obvious from the XCTD data by examining the density inversions (loop shapes of the temperature–salinity profile). For the subarctic North Pacific, however, the salinity error is found in the seasonal thermocline without density inversions (Fig. 5). In the region of a strong vertical temperature gradient (>0.2 °C m^{-1}) between 20 and 40 m depth, the XCTD salinity was systematically lower than the CTD salinity observed at a neighboring station. The temperature–salinity profile from the corrected XCTD data, which incorporates an advance of 1.5 scans of the conductivity data, shows an almost straight line between 20 and 60 m depth, similar to the CTD data. The difference in the average salinity from the surface to 100 m depth between the original and corrected XCTD data was –0.015 (Fig. 5). Although the magnitude of the error is smaller than the manufacturer's specification (0.042; Table 1), it is one-quarter of the surface-layer salinity change (–0.057) recorded in the subpolar North Pacific during recent decades (Hosoda et al. 2009), and this systematic error must be removed for climate change research.

d. Salinity calculations

For the XCTD salinity calculation, pressure was estimated from the XCTD data and location (latitude) as follows.

$$P_{i+1} = P_i + (\rho_{i+1} + \rho_i)\,(g_{i+1} + g_i)\,(Z_{i+1} - Z_i)/4, \qquad (3)$$

where P is pressure, ρ is density, and g is gravitational acceleration. ρ is a function of pressure, temperature, and salinity, and g is a function of pressure and latitude (Fofonoff and Millard 1983). At the sea surface, P_0 and Z_0 are zero. Temperature and conductivity data for just beneath the sea surface were assigned the same values as the shallowest valid data. For the calculation of ρ_{i+1} and g_{i+1}, the pressure of P_i was used as an approximation since the error induced by this approximation is negligible. XCTD salinity was calculated from the estimated pressure, temperature, and conductivity by using the reference conductivity of 42.896 mS cm^{-1} at a salinity of 35, temperature of 15 °C, and pressure of 0 dbar. This reference conductivity value is used in the manufacturer's data processing software.

The salinity calculation is done in the same manner by the manufacturer's data processing software for the MK-130 system. However, for the MK-100, salinity is calculated by using depth instead of pressure. Because the pressure is about 1% greater than the depth at depths less than 1000 m, a depth-dependent systematic error exists in the salinity data from the MK-100 (e.g., the salinity error at 1000 m depth was about +0.006 at 47°N compared to +0.004 at 16°S). Although the magnitude of the error is again much less than the manufacturer's specification (Table 1), it is much greater than the observed salinity change (0.002) in the eastern South Pacific Antarctic Intermediate Water between 1992 and 2003 (Schneider et al. 2005), and this systematic error must be removed for climate change research.

e. Offset correction of salinity data

For the deep ocean, changes in salinity in time and space may often be much smaller than the XCTD salinity error, and the XCTD salinity offset correction is effective in such cases. If temperature–salinity relationships are known, or appropriate CTD data are available for the observed region, the XCTD salinity data can be corrected with sufficient accuracy (Itoh and Shimada 2003; Uchida and Imawaki 2008). For the XCTD salinity data used in this study, salinity offset errors were estimated from deep-water temperature–salinity relationships obtained from the CTD data (Table 3). The bias-corrected XCTD data should be used for climate change research.

4. Evaluation of the depth error

Depth determination may be the most likely source of error in XCTD data. To evaluate the depth error in the XCTD data, a temperature-error-free method should be used, as documented in previous studies (Hanawa et al. 1995; Kizu et al. 2008). To remove the bias-like temperature error, the large vertical scale temperature structure, and the small vertical scale noise, the individual temperature profiles of XCTD and CTD pairs were band-pass filtered by subtracting temperature profiles low-pass filtered by the running mean filter with a window of 81 m from those with a window of 31 m (Fig. 6). The obtained high-wave number temperature profiles of the XCTD and CTD pairs have a similar pattern, although differences in depth (e.g., about 20 m at 1600 m depth) are evident in the profiles from cruise MR09-01.

We assumed that the XCTD depth error is constant over a range of ±100 m depth, and we estimated the XCTD depth bias that maximized the correlation coefficient between the CTD and XCTD temperature within a specified depth range (±100 m), at 100-m intervals. The estimated depth biases were averaged for each depth, cruise, and probe type (Fig. 7). Although the results for cruises KH-02-3 and MR09-01 are within the manufacturer's specifications, the XCTD depths for cruise MR09-01 were significantly underestimated for both XCTD-1 and XCTD-2 (Fig. 7b). If the error is caused by a discrepancy between coefficient *a* in the fall-rate equation and true terminal velocity, the error of coefficient *a* can be estimated from the regression line. The estimated error of the terminal velocity was –0.0428 m s^{-1} for cruise MR09-01.

5. Discussion

Grounding depths of the XCTD were compared with bottom depths measured by the ship's multi narrow-beam echo sounder during cruise MR09-01 (Murata et al. 2009). The echo sounding data were corrected by using sound velocity profiles calculated from the CTD data, and the data were gridded with a resolution of 0.00125° (about 133 m) for both longitude and latitude and then interpolated for the location where the XCTD was deployed (Fig. 8). Differences between the grounding depth of the XCTD and the echo sounding depth were similar to the differences between the grounding depth of the XCTD and the bottom depth estimated from the maximum depth of the CTD plus the height above the bottom as measured by the altimeter attached to the CTD package. These differences were consistent with the depth error of the XCTD estimated from the regression line in Fig. 7.

Nonuniformity in weight of the XCTD probes may change the terminal velocity of the probe. Assuming that the terminal velocity error is caused by a weight discrepancy between the actual weight of the probe and the weight specified by the manufacturer, the weight discrepancy is calculated to be about 8–9 g less than the normal probe in sea water by using a bulk dynamic model for a vertically falling probe (Green 1984). However, all of the XCTD probes were weighed in air by the manufacturer before they were shipped (Tsurumi-Seiki, personal communication 2009) and were listed as 1068 ± 1 g for the XCTD-1 and 1076 ± 1 g for the XCTD-2. Moreover, the XCTD-1 probes produced in 2003 and the XCTD-2 probes produced in 2008 showed a similar depth error, suggesting that the depth error is not caused by nonuniformity of the products.

Differences in the ambient water temperature may change the terminal velocity by changing the viscous drag. Temperature-dependent coefficients for the XCTD have been proposed by Kizu et al. (2008). However, the difference between the original depth data for the XCTD obtained during cruise MR09-01 and the depth calculated by using temperature-dependent coefficients of the fall-rate equation proposed by Kizu et al. (2008) is less than 4 m. Moreover, ambient temperature profiles for cruise MR09-01 and KH-02-3 are similar. Therefore, the depth error cannot be explained by differences in the ambient temperature.

The terminal velocity for the XCTDs deployed during cruise MR09-01 must be less than that during cruise KH-02-3 because gravitational acceleration is less in lower latitudes. However, the difference (–0.0015 m s^{-1}) in the terminal velocity caused by the difference in gravitational acceleration is much less than the terminal velocity error (–0.0428 m s^{-1}) estimated in Section 4.

Although the systematic depth error is less than the manufacturer's specification, it must be taken into consideration for climate change research; the magnitude of the steric height error (about –1 cm) caused by the depth error of the XCTD is comparable to the magnitude of the steric height rise (2.8 ± 0.9 cm per decade) south of Japan (Uchida and Imawaki 2008). However, more work is needed to clarify the cause of the systematic depth error of the XCTD for cruise MR09-01. In future studies we must keep in mind that XBT/XCTD observations may have similar depth errors and that simultaneous CTD observations are needed to evaluate these errors.

Acknowledgments

We are grateful to the technicians of Global Ocean Development Inc. who conducted the XCTD and the multi narrow-beam echo sounder observations during cruise MR07-04 and MR09-01 leg 1 and 2. The XCTD observations during cruise KH-02-3 leg 1 were jointly carried out by Shiro Imawaki (Japan Agency for Marine-Earth Science and Technology), Kaoru Ichikawa (Research Institute for Applied Mechanics, Kyushu University), Tomowo Watanabe (National Research Institute of Fisheries Science, Yokohama, Japan), and Tsurumi Seiki Co., Ltd.

References

Fofonoff, N. P. and R. C. Millard Jr., 1983: Algorithms for computation of fundamental properties of seawater. Unesco technical papers in marine science, **44**, 53 pp.

Gille, S. T., A. Lombrozo, J. Sprintall and G. Stephenson, 2009: Anomalous spiking in spectra of XCTD temperature profiles. *J. Atmos. Oceanic Technol.*, **26**, 1157–1164.

Gouretski, V. and K. P. Koltermann, 2007: How much is the ocean really warming?. *Geophys. Res. Lett.*, **34**, L01610, doi:10.1029/2006GL027834.

Green, A. W., 1984: Bulk dynamics of the expendable bathythermograph (XBT). *Deep-Sea Res.*, **31**, 415–426.

Hanawa, K., P. Rual, R. Bailey, A. Sy and M. Szabados, 1995: A new depth-time equation for Sippican or TSK T-7, T-6 and T-4 expendable bathythermographs (XBT). *Deep-Sea Res. I*, **42**, 1423–1451.

Hosoda, S., T. Suga, N. Shikama and K. Mizuno, 2009: Global surface layer salinity change detected by Argo and its implication for hydrological cycle intensification. *J. Oceanogr.*, **65**, 579–586.

Itoh, M. and K. Shimada, 2003: XCTD salinity calibration in the Arctic Ocean, *JAMSTECR*, **48**, 107–113 (in Japanese with English abstract).

Johnson, G. C., 1995: Revised XCTD fall-rate equation coefficients from CTD data. *J. Atmos. Oceanic Technol.*, **12**, 1367–1373.

Kawano, T., M. Aoyama, T. Joyce, H. Uchida, Y. Takatsuki and M. Fukasawa, 2006: The latest batch-to-batch difference table of standard seawater and its application to the WOCE onetime sections. *J. Oceanogr.*, **62**, 777–792.

Kawano, T., H. Uchida and T. Doi, 2009: *WHP P01, P14 Revisit Data Book*, 212 pp., Japan Agency for Marine-Earth Science and Technology, Yokosuka, Kanagawa, Japan.

Kizu, S. and K. Hanawa, 2002: Start-up transient of XBT measurement. *Deep-Sea Res. I*, **49**, 935–940.

Kizu, S., H. Onishi, T. Suga, K. Hanawa, T. Watanabe and H. Iwamiya, 2008: Evaluation of the fall rates of the present and developmental XCTDs. *Deep-Sea Res. I*, **55**, 571–586.

Koso, Y., H. Ishii and M. Fujita, 2005: An examination of the depth conversion formula of XCTD-2F. *Technical Bulletin on Hydrology and Oceanography*, 23, 93–98 (in Japanese).

Mizuno, K. and T. Watanabe, 1998: Preliminary results of in-situ XCTD/CTD comparison test. *J. Oceanogr.*, **54**, 373–380.

Murata, A., H. Uchida and K. Sasaki, 2009: R/V Mirai Cruise Report, MR09-01, http://www.godac.jamstec.go.jp/cruisedata/mirai/e/MR09-01_leg1.html.

Schneider, W., M. Fukasawa, H. Uchida, T. Kawano, I. Kaneko and R. Fuenzalida, 2005: Observed property changes in eastern South Pacific Antarctic Intermediate Water. *Geophys. Res. Lett.*, **32**, L14602, doi:10.1029/2005GL022801.

Uchida, H. and S. Imawaki, 2008: Estimation of the sea level trend south of Japan by combining satellite altimeter data with in situ hydrographic data. *J. Geophys. Res.*, **113**, C09035, doi:10.1029/2008JC004796.

Uchida, H., S. Imawaki, H. Ichikawa and the ASUKA Group, 2008: ASUKA Hydrographic Data Collection, *Reports of Research Institute for Applied Mechanics, Kyushu University*,

135, 21–31.

Uchida, H., K. Ohyama, S. Ozawa and M. Fukasawa, 2007: In situ calibration of the SeaBird 9*plus* CTD thermometer, *J. Atmos. Oceanic Technol.*, **24**, 1961–1967.

Uehara, K., S. Kizu, K. Hanawa, Y. Yoshikawa and D. Roemmich, 2008: Estimation of heat and freshwater transports in the North Pacific using high-resolution expendable bathythermograph data, *J. Geophys. Res.*, **113**, C02014, doi:10.1029/2007JC004165.

Wijffels, S. E., J. Willis, C. M. Domingues, P. Barker, N. J. White, A. Gronell, K. Ridgway and J.A. Church, 2008: Changing expendable bathythermograph fall rates and their impact on estimates of thermosteric sea level rise. *J. Climate*, **21**, 5657–5672.

Figure captions

Figure 1. Locations of XCTD casts in the Kuroshio south of Japan (KH-02-3), the subarctic North Pacific (MR07-04), and the subtropical South Pacific (MR09-01). Dots and circles indicate locations of XCTD-1 and XCTD-2, respectively. The manufacture year of the XCTD probes is shown in parentheses.

Figure 2. Comparison of temperature–salinity profiles from (a) XCTD raw data, (b) XCTD data with anomalous spikes at frequencies of 5 and 10 Hz removed, (c) XCTD data low-pass filtered by the running mean with a window of 15 scans (about 2 m), and (d) CTD data averaged over 1 dbar. The profiles are shown with salinity offsets to prevent overlap.

Figure 3. High-pass-filtered XCTD temperature (solid line) and conductivity (dotted line) profiles. The profiles were high-pass filtered by subtracting profiles low-pass filtered by the running mean with a window of 10 m (75 data points) from the original profiles. To remove noise, the original profiles were low-pass filtered first by the running mean with a window of 2 m (15 data points). Data were obtained from just north of the Kuroshio axis.

Figure 4. Comparison of temperature (solid lines) and salinity (dotted lines) profiles from CTD and XCTD data obtained at the same station as that for Fig. 3. Mismatch of the response time of the XCTD temperature and conductivity data was compensated for by delaying the 25 Hz XCTD conductivity data relative to the temperature by 1, 1.5, and 2 scans. The profiles are

shown with horizontal offsets to prevent overlap. The XCTD salinity profile calculated by using the conductivity data aligned by 1.5 scans agrees well with the CTD salinity profile.

Figure 5. Comparison of temperature–salinity profiles of CTD (thin line) and XCTD (dotted line) data obtained in the subarctic North Pacific. The XCTD profile corrected for the mismatch of the response time is also shown (thick line). Dots indicate the data at 20, 40, 60, and 100 m depths. Contour lines indicate the potential density anomaly (kg m^{-3}).

Figure 6. Comparisons of band-pass-filtered temperature profiles between CTD (solid lines) and XCTD (dotted lines) for (a) KH-02-3 and (b) MR09-01. The profiles were band-pass filtered by subtracting profiles low-pass filtered by the running mean with a window of 81 m from the profiles low-pass filtered by the running mean with a window of 31 m.

Figure 7. Differences between the XCTD and CTD depths for (a) KH-02-3 and (b) MR09-01. Filled and open circles are for XCTD-1 and XCTD-2, respectively. The differences were estimated from the comparisons of the band-pass-filtered temperature profiles (see text for detail). The horizontal bars indicate standard deviation of the estimates. The dotted lines indicate the manufacturer's specification for the XCTD depth error. The dashed line in (b) is the regression line for the XCTD-2 data.

Figure 8. Differences between bottom depth estimated from XCTD data and that measured by

the ship's multi narrow-beam echo sounder (MNBES) for cruise MR09-01 (the open triangle for XCTD-1 and the open circles for XCTD-2). Differences between the XCTD bottom depth and bottom depth estimated from the CTD with altimeter data are also shown (the filled triangle for XCTD-1 and the filled circles for XCTD-2). The dashed line indicates the XCTD depth error estimated from the regression line in Fig. 7.

Table 1. Manufacturer's specifications for the XCTD-1 and XCTD-2. Accuracy of the calculated salinity was estimated from the root-sum-square of 0.021 from the temperature error, 0.035 from the conductivity error, and 0.010 from the pressure error at a depth of 1000 m, a temperature of 4 °C, and conductivity of 32.5 mS cm^{-1} (calculated salinity of about 34.4).

Parameter	Range	Accuracy
Temperature	–2 to 35 °C	0.02 °C
Conductivity	0–60 mS cm^{-1}	0.03 mS cm^{-1}
Depth	0–1000 m (for XCTD-1)	5 m or 2%, whichever is greater
	0–1850 m (for XCTD-2)	5 m or 2%, whichever is greater
(Salinity)		0.042

Table 2. Manufacturer's coefficients for the fall-rate equation (equation 1 in text).

Model	*a* (Terminal velocity, m s^{-1})	*b* (Acceleration, m s^{-2})	Source
XCTD-1	3.42543	0.00047	Mizuno and Watanabe (1998)
XCTD-2	3.43898	0.00031	Koso et al. (2005)

Table 3. XCTD salinity bias estimated from deep-water temperature–salinity relationships. The depth error for the XCTD data from cruise MR09-01 was corrected (see Section 4 for more detail), and the salinity biases were then estimated.

Cruise	Number of profiles	Average	Standard deviation
KH-02-3	16	0.004	0.018
MR07-04	16	–0.018	0.009
MR09-01	29	–0.019	0.011
Total	61	–0.013	0.016

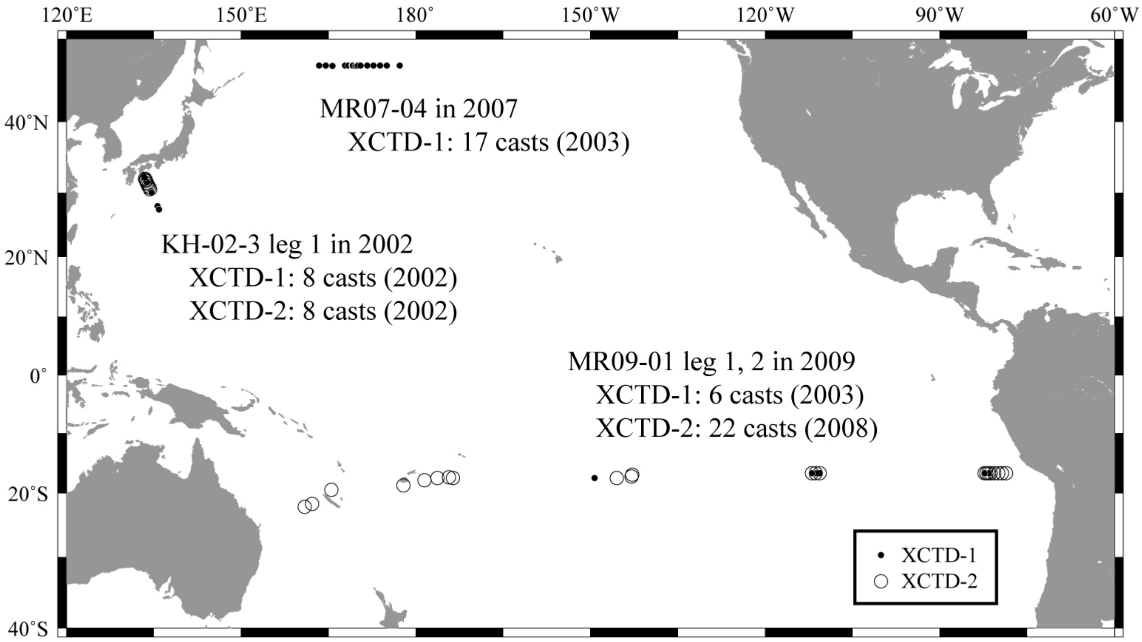

Figure 1. Locations of XCTD casts in the Kuroshio south of Japan (KH-02-3), the subarctic North Pacific (MR07-04), and the subtropical South Pacific (MR09-01). Dots and circles indicate locations of XCTD-1 and XCTD-2, respectively. The manufacture year of the XCTD probes is shown in parentheses.

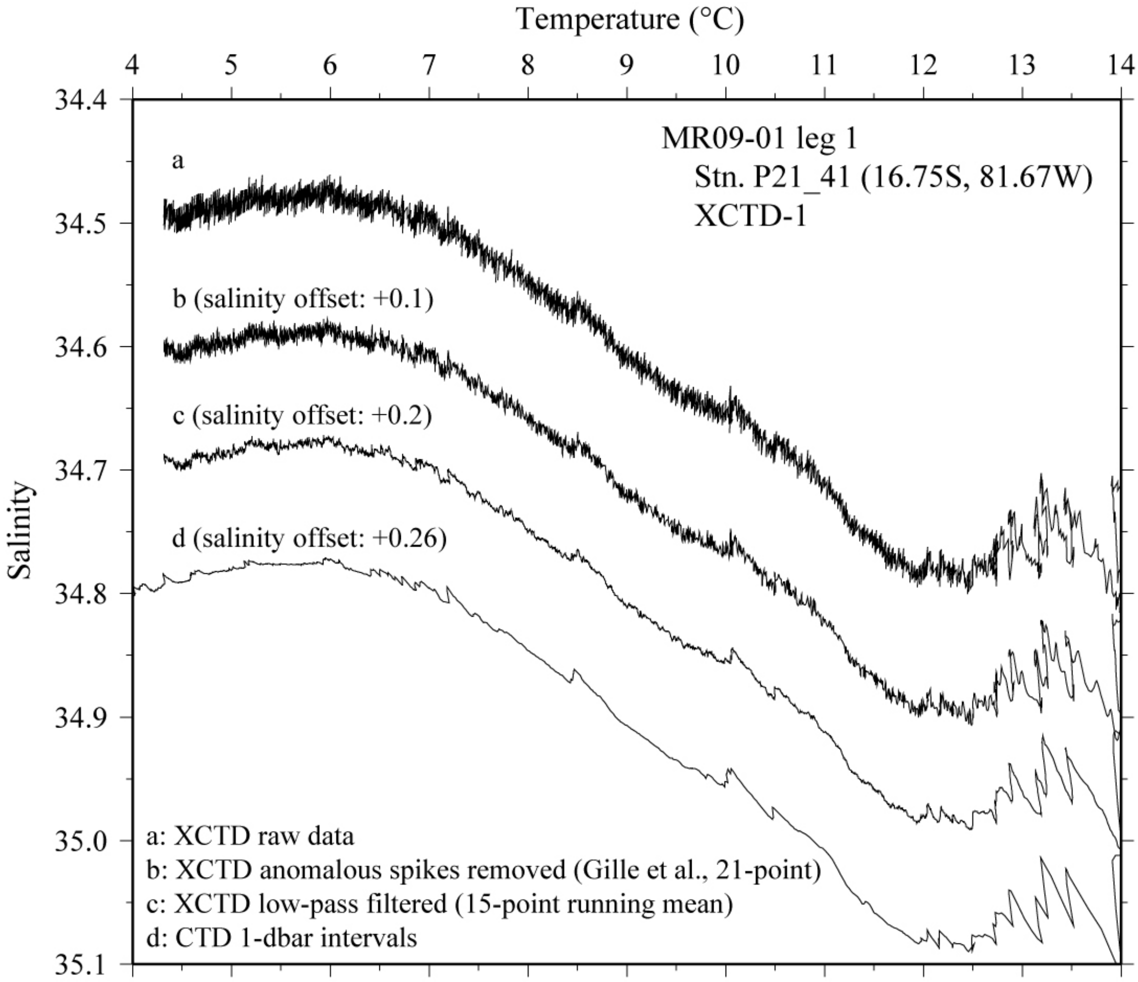

Figure 2. Comparison of temperature–salinity profiles from (a) XCTD raw data, (b) XCTD data with anomalous spikes at frequencies of 5 and 10 Hz removed, (c) XCTD data low-pass filtered by the running mean with a window of 15 scans (about 2 m), and (d) CTD data averaged over 1 dbar. The profiles are shown with salinity offsets to prevent overlap.

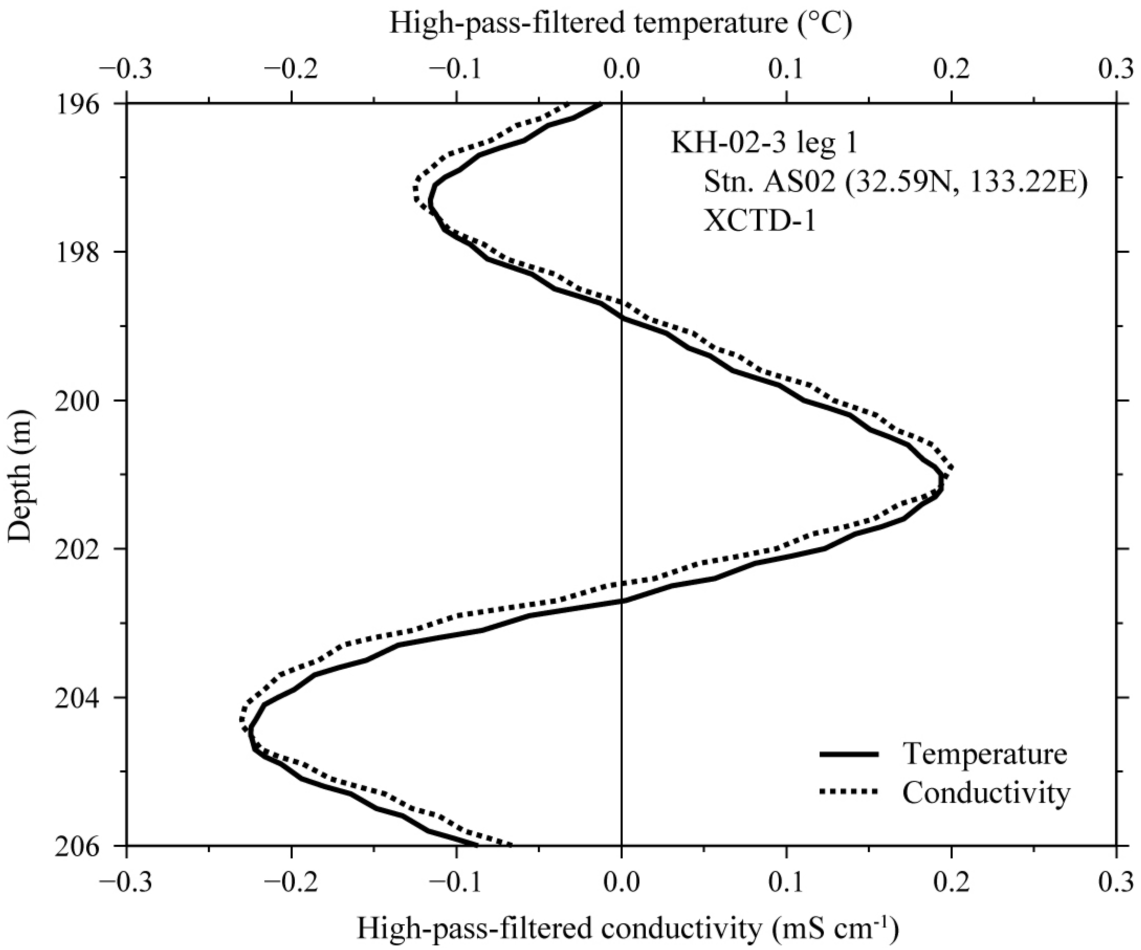

Figure 3. High-pass-filtered XCTD temperature (solid line) and conductivity (dotted line) profiles. The profiles were high-pass filtered by subtracting profiles low-pass filtered by the running mean with a window of 10 m (75 data points) from the original profiles. To remove noise, the original profiles were low-pass filtered first by the running mean with a window of 2 m (15 data points). Data were obtained from just north of the Kuroshio axis.

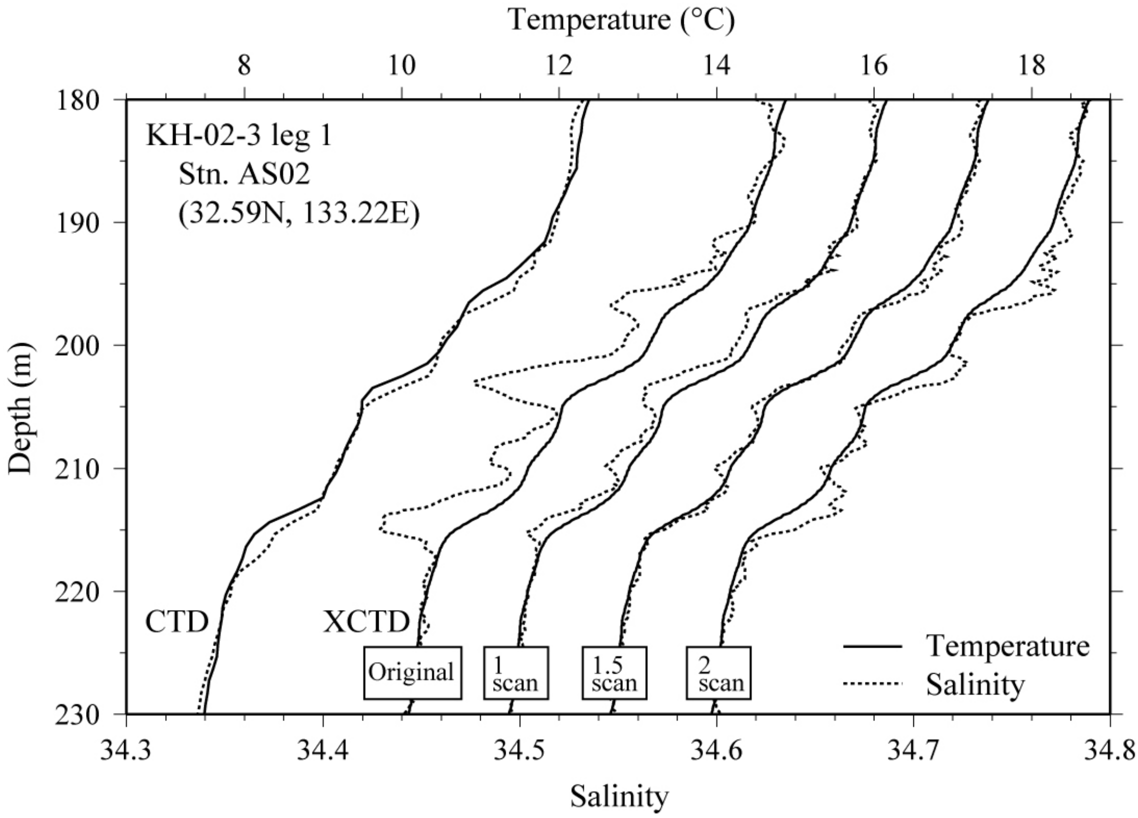

Figure 4. Comparison of temperature (solid lines) and salinity (dotted lines) profiles from CTD and XCTD data obtained at the same station as that for Fig. 3. Mismatch of the response time of the XCTD temperature and conductivity data was compensated for by delaying the 25 Hz XCTD conductivity data relative to the temperature by 1, 1.5, and 2 scans. The profiles are shown with horizontal offsets to prevent overlap. The XCTD salinity profile calculated by using the conductivity data aligned by 1.5 scans agrees well with the CTD salinity profile.

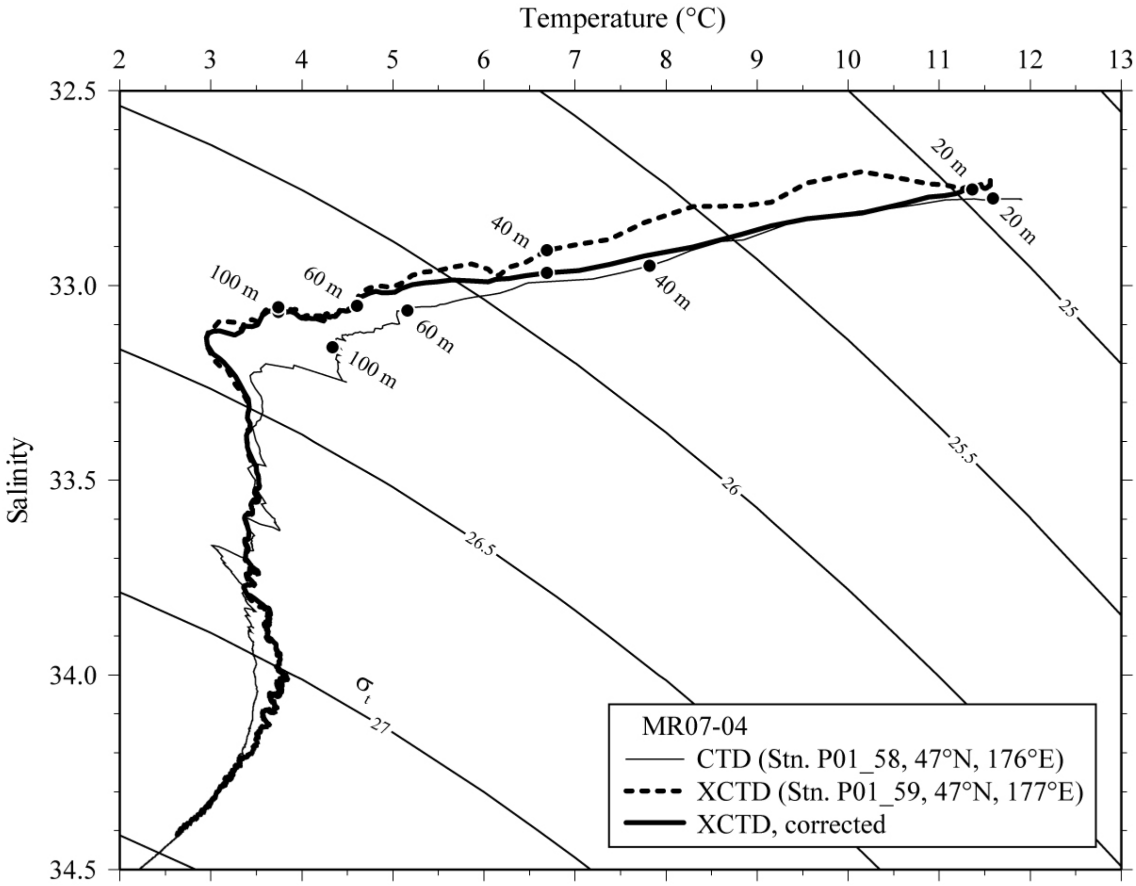

Figure 5. Comparison of temperature–salinity profiles of CTD (thin line) and XCTD (dotted line) data obtained in the subarctic North Pacific. The XCTD profile corrected for the mismatch of the response time is also shown (thick line). Dots indicate the data at 20, 40, 60, and 100 m depths. Contour lines indicate the potential density anomaly (kg m^{-3}).

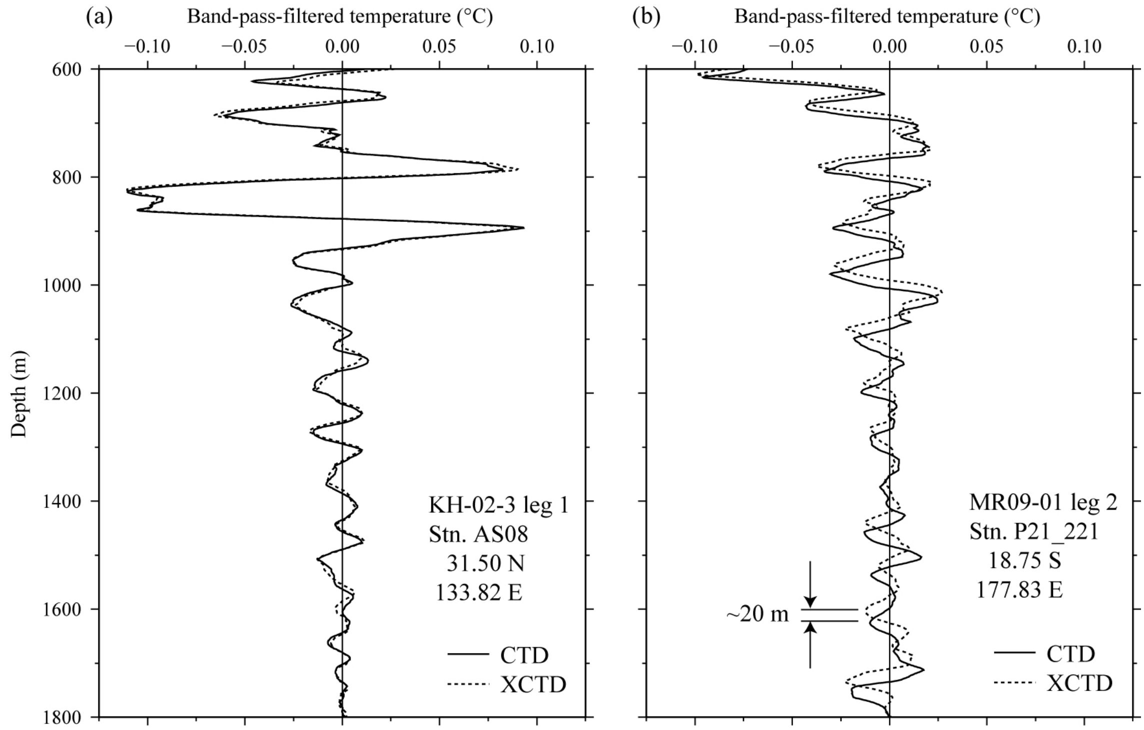

Figure 6. Comparisons of band-pass-filtered temperature profiles between CTD (solid lines) and XCTD (dotted lines) for (a) KH-02-3 and (b) MR09-01. The profiles were band-pass filtered by subtracting profiles low-pass filtered by the running mean with a window of 81 m from the profiles low-pass filtered by the running mean with a window of 31 m.

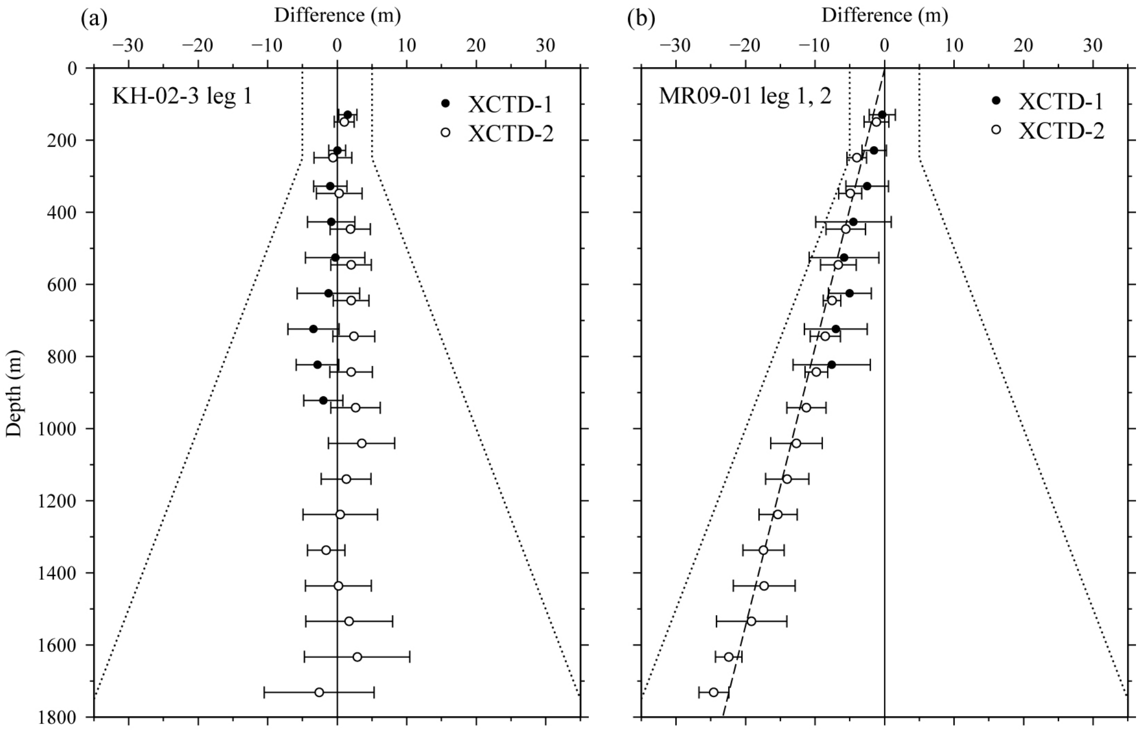

Figure 7. Differences between the XCTD and CTD depths for (a) KH-02-3 and (b) MR09-01. Filled and open circles are for XCTD-1 and XCTD-2, respectively. The differences were estimated from the comparisons of the band-pass-filtered temperature profiles (see text for detail). The horizontal bars indicate standard deviation of the estimates. The dotted lines indicate the manufacturer's specification for the XCTD depth error. The dashed line in (b) is the regression line for the XCTD-2 data.

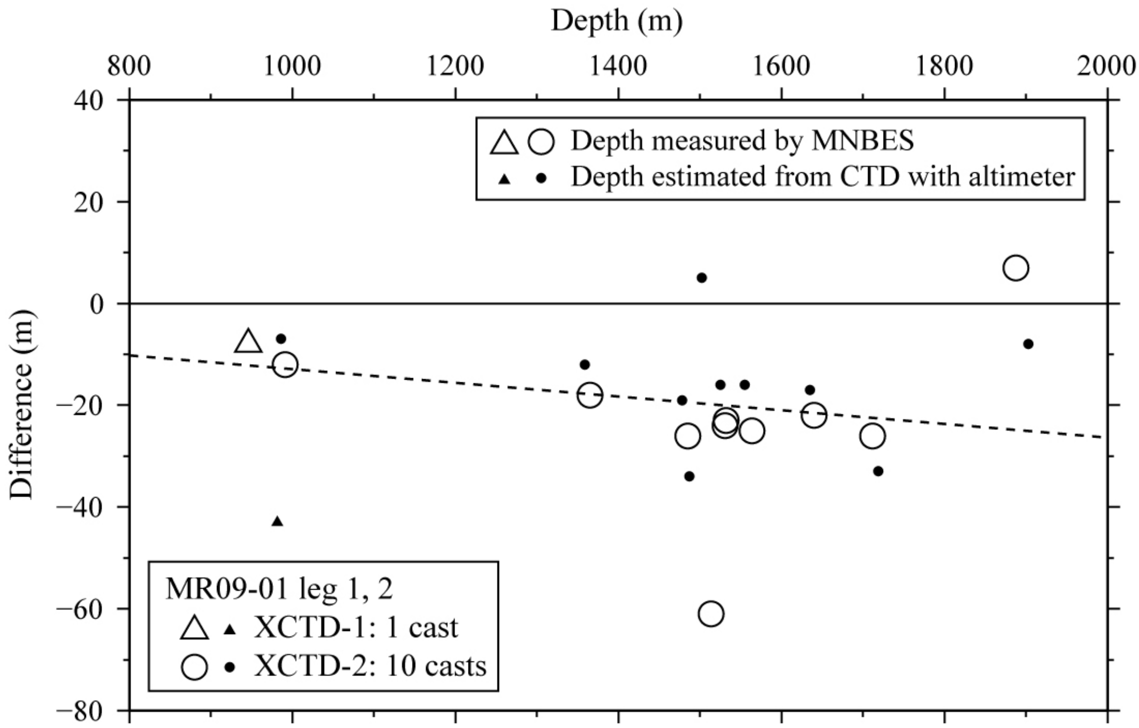

Figure 8. Differences between bottom depth estimated from XCTD data and that measured by the ship's multi narrow-beam echo sounder (MNBES) for cruise MR09-01 (the open triangle for XCTD-1 and the open circles for XCTD-2). Differences between the XCTD bottom depth and bottom depth estimated from the CTD with altimeter data are also shown (the filled triangle for XCTD-1 and the filled circles for XCTD-2). The dashed line indicates the XCTD depth error estimated from the regression line in Fig. 7.